Biological Trace Element Research (2023) 201:2811–2822
https://doi.org/10.1007/s12011-022-03369-2

Inhibition of H1N1 Influenza Virus-induced Apoptosis by Ebselen Through ROS-mediated ATM/ATR Signaling Pathways

Danyang Chen[1] · Ruilin Zheng[1] · Jingyao Su[1] · Jia Lai[1] · Haitian Chen[1] · Zhihui Ning[1] · Xia Liu[1] · Bing Zhu[1] · Yinghua Li[1]

Received: 24 May 2022 / Accepted: 23 July 2022 / Published online: 27 July 2022

Abstract

Influenza A viruses can cause global outbreaks and seasonal pandemics. However, the use of conventional anti-influenza drugs leads to an increase in drug-resistant mutations in influenza viruses worldwide. Therefore, numerous studies have focused on developing effective anti-influenza drugs. It is feasible to treat influenza by targeting influenza-mediated oxidative damage. Ebselen is a synthetic organoselenium compound which provides glutathione peroxidase-like activity. It has been shown to play a role in anti-influenza therapy, but the mechanism remains to be further explored. This experiment verified the anti-influenza effect of ebselen. CCK-8 and PCR showed that ebselen had a significant inhibitory effect on virus replication compared with the virus group. In addition, the mechanistic investigations revealed that ebselen could inhibit influenza-mediated apoptosis, mitochondrial damage, accumulation of reactive oxygen species, and DNA breakage. At the same time, ebselen significantly inhibited the phosphorylation of ATM and ATR and promoted the activation of PARP and Caspase-3. Ebselen, on the other hand, reduced the inflammatory response caused by influenza. These results suggest that ebselen is a promising inhibitor for H1N1.

Keywords Influenza · Ebselen · Oxidative damage · Apoptosis · Mechanism

Introduction

Influenza virus (IV) is a spherical, 80–120 nm in diameter enveloped virus containing 7 or 8 independent single-stranded negative RNA gene segments [1]. Influenza can be divided into four types, influenza A, influenza B, influenza C, and influenza D, according to the antigenicity differences of nuclear protein (NP) and matrix protein (MP) of the virus on its surface [2]. According to the World Health Organization, about 4 million cases of severe infection and about 500,000 deaths occur every year [3]. The main epidemic strains of influenza viruses include influenza A and B, which cause epidemics of varying severity each year. Influenza A virus (IAV) infection may lead to pneumonia and even acute respiratory failure, which poses a serious threat to human health [4]. Currently, vaccination and drug treatment are used to prevent and treat influenza, respectively. However, influenza virus vaccines do not provide adequate protection due to the rapid mutation of virus epitopes targeted by the vaccine [5]. Because targeted vaccines take a long time to develop, vaccination is not the best way to protect against influenza [6]. Currently available anti-influenza virus drugs include Amantadine, Rimantadine, Oseltamivir, Zanamivir, and Peramivir, all of which target the life cycle of the virus. Amantadine and Rimantadine are M2 protein ion channel inhibitors, which block the M2 ion channel of influenza A virus, preventing the virus from uncoating and releasing viral RNA [7]. Oseltamivir, Zanamivir, and Peramivir are neuraminidase inhibitors that block viral dissociation from sialic acid residues, thereby preventing the release of new viral particles [8]. However, more and more influenza strains have become resistant to drugs in the past few years [9, 10]. During the 2008–2009 pandemic, countries such as the USA, Canada, the United Kingdom, and Australia found high proportions (> 90%) of Oseltamivir-resistant influenza

Danyang Chen, Ruilin Zheng and Jingyao Su contributed equally to this work.

✉ Yinghua Li
liyinghua@gzhmu.edu.cn

[1] Center Laboratory, Guangzhou Women and Children's Medical Center, Guangzhou Medical University, Yuexiu District, No 318 Renminzhong Road, Guangzhou 510120, China

A H1N1 strains [11]. The problem of drug resistance makes it difficult to treat the influenza virus in a clinic. Therefore, it is essential to constantly develop effective antiviral drugs against influenza viruses.

Cells often produce reactive oxygen species (ROS) during IAV infection [12], thus promoting cell apoptosis, lung injury, and inflammation. ROS plays an important role in IAV infection, which may have implications for therapy. Mitochondria are involved in ROS production during oxidative phosphorylation [13]. The rate of mitochondrial ROS production is regulated by mitochondrial membrane potential. At the same time, excessive ROS would mediate mitochondrial permeability transition pore (mPTP) opening for a long time, leading to ROS explosion and even mitochondrial damage [14]. Mitochondrial damage promotes Ca^{2+} and cytochrome C and causes Caspase-9 to activate Caspase-3/6/7. In addition, mitochondrial damage can decouple the mitochondrial electron transport chain, down-regulate ATP production level, up-regulate the expression level of pro-apoptotic protein Bax, and finally lead to cell apoptosis. On the other hand, excessive ROS can damage growth factors, transcription factors, proteins, nucleic acids, sugars, lipids, and other biomolecules [15]. Previous studies of our research group have shown that influenza infection can induce mitochondrial damage, leading to the overproduction of ROS. The accumulation of ROS can lead to the damage of nucleic acid in cells, activate Caspase-3, and activate the apoptosis signaling pathway [16, 17]. Meanwhile, the infection of influenza induces the innate immune system to produce inflammatory cytokines, which may mediate a severe inflammatory response [18]. Therefore, in addition to viral components, the therapeutic treatment of influenza virus infection may be achieved by targeting virus-induced ROS and redox-associated responses. Targeting intracellular redox responses may suppress the propagation of IAV and reduce inflammation in the host.

Ebselen [2-phenyl-1, 2-benzisoselenazol-3(2*H*)-one] is a synthetic organic selenium compound with glutathione peptide peroxidase activity [19]. Owing to its antioxidant properties, ebselen can protect cells from oxidation and free radical damage and has been used as an effective tool for studying redox-related mechanisms. Ebselen also has an impact on antiviral therapy. For example, ebselen reduced Zika-induced testicular oxidative stress, leukocyte infiltration, and pro-inflammatory responses [20], alleviated influenza A virus-induced pulmonary inflammatory response [21], and targeted Mpro, a key enzyme for the replication of COVID-19 virus [22]. These studies revealed that ebselen has certain antiviral effects. However, the mechanism by which ebselen inhibits the influenza virus and reduces inflammation remains to be further elucidated. The purpose of this study was to further understand the anti-influenza mechanism of ebselen by observing the effect of ebselen on MDCK cells infected with the influenza A virus. CCK-8 and PCR were used to evaluate the toxicity and antiviral effect of ebselen. It was confirmed by cell cycle and Annexin-V assay that ebselen inhibited influenza-mediated apoptosis. Studies on the mechanism of ebselen inhibiting influenza-mediated apoptosis showed that ebselen improved influenza-induced mitochondrial membrane potential decline and inhibited ROS accumulation and nucleic acid rupture. Western blot showed that ebselen regulated the expression of apoptosis-related proteins and inhibited influenza-mediated apoptosis. On the other hand, ebselen also inhibited the release of intracellular pro-inflammatory factors and alleviated influenza-mediated inflammation.

Materials and Methods

Materials

Madin-Darby canine kidney cells (MDCK) were obtained from American Type Culture Collection (ATCC CCL-34TM, Rockville, USA). H1N1 influenza virus was isolated from clinical samples of Guangzhou Women and Children's Medical Center, Guangzhou Medical University (Guangzhou, China). Fetal bovine serum (FBS), pancreatic enzymes, and Dulbecco's modified Eagle's medium (DMEM) were purchased from Gibco (California, USA). P-ATM, P-ATR, PARP, Cleaved PARP, Caspase-3, Cleaved Caspase-3, and β-actin antibodies were purchased from Cell Signaling Technology (Boston, USA). Cell counting kit-8 (CCK-8 kit), reverse transcription-polymerase chain reaction kit (RT-PCR kit), JC-1 Mitochondrial Membrane Potential Assay Kit, Cell Cycle Assay Kit, Annexin-V-Propidium iodide (PI) Co-staining Kit, and Enhanced Chemiluminescence (ECL) Assay Kit were obtained from Beyotime Biotechnology (Shanghai, China). Tunel, 4′, 6-diamidino-2-phenylindole (DAPI), and 2′, 7′-dichlorofluorescein diacetate (DCF-DA) were purchased from Sigma-Aldrich (St. Louis, USA). The detection of the cells and the cytokine were derived from the BD FACSCanto II flow cytometer (Franklin Lakes, USA). Ebselen was provided by Tianfeng Chen, College of Chemistry and Materials Science, Jinan University (Guangzhou, China).

Cell Culture and Virus Infection

MDCK cells were incubated in DMEM with 10% FBS, 100 U/mL penicillin, and 50 U/mL streptomycin in a carbon dioxide cell incubator at a constant temperature of 37 ℃ with 5% CO_2. MDCK cells were infected with H1N1, and the median tissue culture infective dose ($TCID_{50}$) was calculated by the Reed–Muench method [23]. MDCK cells were cultured to a cell density of 80–90% and then adsorbed with

the H1N1 virus for 2 h. After that, the remaining virus was discarded, and the cells were added to the virus-maintaining medium [24]. The virus-maintaining medium was DMEM containing 2 μg/mL TPCK-treated trypsin. After the titer of H1N1 was determined, the H1N1 virus was used for in vitro study at the titer of 100 $TCID_{50}$/0.1 mL [25].

Cell Counting Kit-8 Assay

CCK-8 assay was used to determine the cytotoxicity and antiviral effect of ebselen. Briefly, cells (1×10^5/mL) were inoculated in a 96-well plate for 24 h. Then, the cells were exposed to ebselen at progressively increased concentrations (4 mM, 8 mM, 16 mM, 32 mM, and 64 mM) for 48 h. After that, 10 μL CCK-8 dye was added to each well and incubated at 37 ℃ for 2 h. The absorbance at 450 nm was measured with a microplate reader. Cytotoxicity was expressed according to the following formula: cytotoxicity (%) = {(Abs sample) − (Abs blank)} / {(Abs negative control) − (Abs blank)} × 100% [26]. To assess the impact of ebselen on virus-induced cell growth, cells were infected with 100 $TCID_{50}$/0.1 mL H1N1 for 2 h prior to ebselen treatment. Then the CCK-8 assay was performed as explained above, after which OD values were measured. The ebselen concentration of 8 mM was selected for subsequent experiments. Each experiment was repeated three times ($n = 3$).

Fluorescence Real-time PCR

MDCK cells were divided into 4 groups: control, H1N1, ebselen, and H1N1 + ebselen. MDCK cells were planted in 6-well plates for 24 h and incubated with H1N1 for 2 h. Then 8 mM ebselen was added into the well for 48 h. Viral proliferation was assessed by fluorescence real-time PCR, and total RNA was extracted by RNA Extraction Kits (Qiagen). ABI7500 system was used in PCR assay, and the $2-\Delta\Delta Ct$ method was applied for calculating gene expression. Primers were as follows: H1N1 forward primer 5′ CTCAGCAAA TCC-TACATTA3′ and reverse primer 5′TAGTAGATGGAT GGTGAAT3′, GAPDH forward primer 5′CGCCAAGAA GGTGATCATTTC3′, and reverse primer 5′CAGGAGGCG TTCGAGATGAC 3′ [27]. Each experiment was repeated three times ($n = 3$).

Cell Cycle Assay

DNA content was measured by flow cytometry to evaluate the impact of ebselen on the cell cycle, and cell apoptosis was detected according to the sub-G1 population in the histogram. MDCK cells were divided into 4 groups and inoculated in 6 cm Petri dishes. After different treatments, the cells were cultured in an incubator at 33 ℃ 5% CO_2 for 48 h, then digested with trypsin and collected. The cells of the four groups were fixed with 70% ethanol at 4 ℃ for 2 h. The supernatant was discarded by centrifugation, and the cells were washed with PBS. Propidium iodide (PI) dye and RNase A were added according to the dosage specified in the instructions, and the cells were incubated at 4 ℃ for 30 min. Twenty thousand cells were detected by flow cytometry using standard procedures, and the cell cycle was analyzed by Modfit software [28]. Each experiment was repeated three times ($n = 3$).

Annexin-V/PI Co-staining Assay

Fluorescein isothiocynate (FITC)-conjugated Annexin-V and propidium iodide (PI) staining was applied to determine the apoptosis of MDCK cells. Briefly, MDCK cells infected with H1N1 were treated with 8 mM ebselen for 48 h. After that, the cells were fixed with 70% ethanol at 4 ℃ for 6 h, and then the apoptotic cells were further detected by the Annexin-V/PI apoptosis kit [29]. The apoptosis rate of cells was recorded by flow cytometry. And the fluorescence intensity of cells was detected by Leica inverted fluorescence microscope. Each experiment was repeated three times ($n = 3$).

Measurement of Mitochondrial Membrane Potential by JC-1 Fluorescence

The reduction of mitochondrial membrane potential is a significant event of apoptosis. The collected cells were co-incubated with JC-1 solution at 37 ℃ for 20 min, then washed with buffer twice and detected by flow cytometry. The ratio of the intensity of red fluorescence to green fluorescence represents the mitochondrial membrane potential [30]. In addition, MDCK cells on the 6-well plate were mixed with 1 mL JC-1 solution and incubated at 37 ℃ for 20 min. Finally, the fluorescence image was captured through a fluorescence microscope. Each experiment was repeated at least three times. Each experiment was repeated three times ($n = 3$).

TUNEL-DAPI Assay

DNA damage in virus-infected MDCK cells after the treatment was assessed by TUNEL-DAPI assay. As previously described, the supernatant of treated cells in a 6-well plate was discarded, and cells were washed with PBS. Next, cells were fixed with 4% pre-chilled paraformaldehyde for 30 min. TUNEL (green fluorescence) was subsequently added for 60 min and DAPI (blue fluorescence) for 15 min at 37 ℃, protected from light. After PBS washing two times, cells were microscopically observed with photo collection.

ROS Generation

Non-fluorescent DCFH-DA freely penetrates via cell membrane into cells and is oxidized into non-penetrating DCFH with green fluorescence by intracellular ROS. Thus, the level of intracellular ROS was measured by fluorescent intensity. Briefly, cells in each group were treated in a 6-well plate as previously mentioned, and DCFH-DA at the final concentration of 10 mmol/L was added, respectively. ROS level was measured by fluorescent microscopy at 37 ℃ for 20 min. The fluorescence of cells seeded in a 96-well plate was assessed by a fluorescent enzyme-labeled instrument at 488 nm and 525 nm wavelengths.

Western Blot

MDCK cells were cultured in a 10 cm dish at a concentration of 8×10^5/mL, incubated with H1N1 for 2 h after 24 h, and treated with ebselen for 48 h. Then the total protein was extracted, and the protein concentration was measured by BCA protein kits. Protein was denatured at 95 ℃ for 10 min and then separated for protein samples by 10% SDS-PAGE gel and transferred into polyvinylidene difluoride membranes. Polyvinylidene difluoride membranes are sealed with 10% BSA for 2 h and incubated overnight with primary antibodies, including P-ATM, P-ATR, PARP, Cleave PARP, Caspase-3, Cleave Caspase-3, and β-actin antibodies. Then the primary antibody was washed off the membrane, and the secondary antibody was incubated for 2 h. At last, protein bands were detected by enhanced chemiluminescent imaging.

Detection of Intracellular Cytokines by Flow Cytometry

Cellular supernatant was collected after centrifugation (3000 rpm, 10 min) to remove cellular fragments. The mixture containing 20 μL microsphere mixture, 20 μL sample solution, and 20 μL mixture of testing antibodies was added into a 96-well filter plate and then incubated in the dark for 2 h (500 rpm). Then, 20 μL PE-labeled streptavidin–phycoerythrin (SA-PE) solution was added into wells at room temperature for 30 min (500 rpm). Finally, corresponding fluorescence was measured using a flow cytometry instrument, and levels of intracellular cytokines in samples were obtained by analyzing the fluorescent intensity of the immune complex. Fluorescent data were collected by BD FACS Diva software, and levels of intracellular cytokines were assessed by FCAP Array 3.0 Analysis Software.

Statistical Analysis

All experiments were repeated at least three times. Data were presented as mean values ± standard deviation. The difference among groups was analyzed using variance analysis, and SPSS13.0 software was used to perform the two-tailed test. $p < 0.05$ (*) was considered statistically significant.

Results

Cytotoxicity and Antiviral Activity of Ebselen

The cytotoxicity and antiviral activity of ebselen were determined by CCK-8. As shown in Fig. 1A, compared with the control group (100%), the cell viability of MDCK with different concentrations of ebselen was 97.83% in the 4 mM group, 100.43% in the 8 mM group, 100.87% in the 16 mM group, 73.43% in the 32 mM group, and 25.32% in the 64 mM group, respectively. On the other hand, as shown in Fig. 1B, cell viability was reduced to 40.92% after cells were infected with H1N1. After treatment with ebselen, the activity of MDCK cells infected with H1N1 increased to 47.59%, 72.18%, 77.16%, and 87.23%. The cell viability of 8 mM, 16 mM, and 32 mM groups was significantly different from that of the H1N1 group. As shown in Fig. 1C, microscopic observations showed that MDCK cells treated with the H1N1 virus had cytoplasmic atrophy, reduced cell connections, and reduced cell numbers. After co-treatment with ebselen, the cell shape of MDCK tended to be normal gradually with the increase of ebselen concentration. The results showed that ebselen could effectively inhibit the changes in cell morphology and viability induced by H1N1.

Inhibition of Viral Replication by Ebselen

In order to evaluate the inhibition of ebselen against viral replication, cells were divided into four groups, including the control group, ebselen group, H1N1 group, and H1N1 + ebselen group. As shown in Fig. 2A, the virus titer of the H1N1 group was significantly higher than that of the other groups. And the level of viral RNA was 17.5% in the H1N1 + ebselen group compared with the H1N1 group. Therefore, the results showed that ebselen could effectively inhibit viral replication.

Cytokine Release Regulated by Ebselen

The changes in the levels of inflammatory mediators after H1N1 infection were measured by immune microspheres to investigate the impact of ebselen on inflammatory responses. The results showed that cells infected with H1N1 activated a signaling cascade that led to the production of

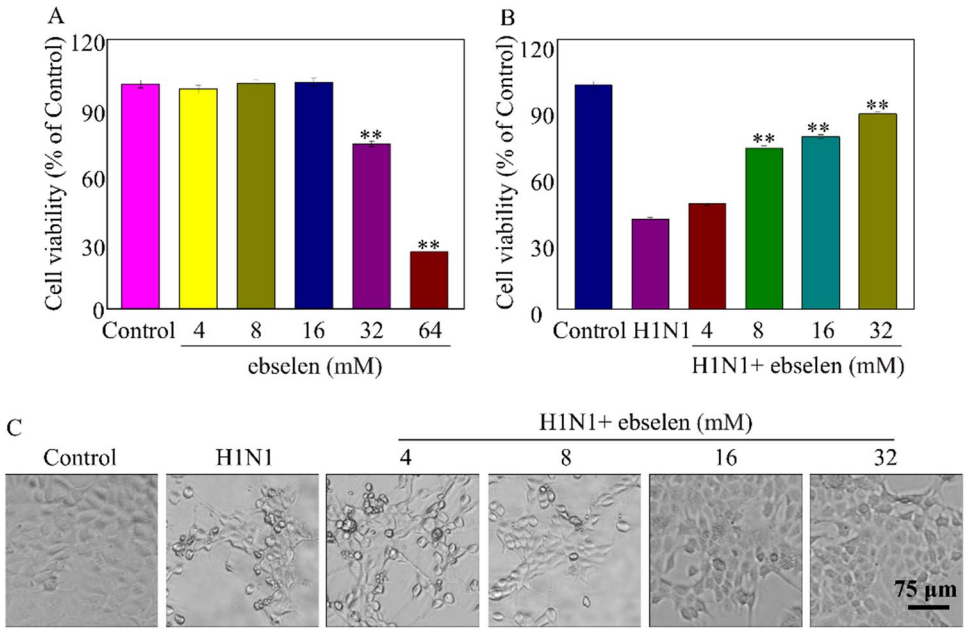

Fig. 1 The cytotoxicity and antiviral effects of ebselen were determined by CCK-8 assay. (**A**) The cytotoxicity of ebselen was determined by the CCK-8 assay. (**B**) Effect of ebselen on the growth of MDCK cells infected with H1N1 was determined by CCK-8 assay. (**C**) Morphological changes of MDCK cells infected with H1N1 were observed by phase contrast microscopy. The titer of H1N1 was 100 $TCID_{50}$/0.1 mL. MDCK cells were infected with H1N1 for 2 h and then treated with ebselen at the corresponding concentration for 48 h. Each experiment was repeated at least three times ($n = 3$)

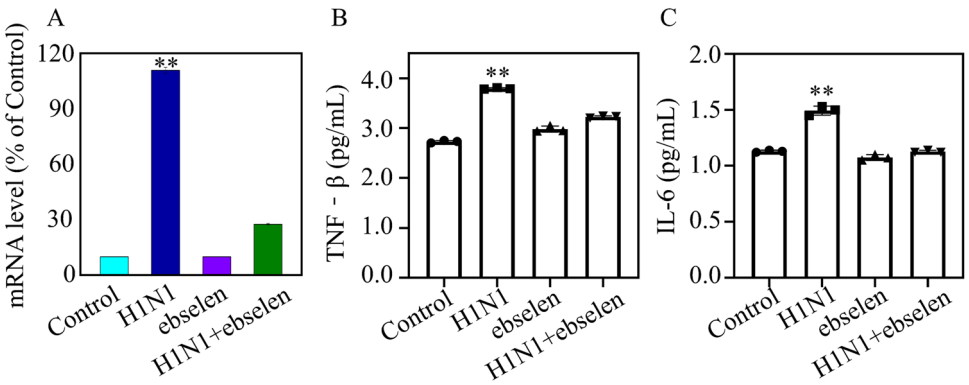

Fig. 2 The replication of H1N1 and the high inflammatory cytokine response mediated by H1N1 were inhibited by ebselen. (**A**) The inhibitory effect of ebselen on H1N1 replication was determined by RT-PCR. (**B**) TNF-β levels of MDCK cells after different treatments were detected by flow cytometry. (**C**) IL-6 levels of MDCK cells after different treatments were detected by flow cytometry. The titer of H1N1 was 100 $TCID_{50}$/0.1 mL. MDCK cells were infected with H1N1 for 2 h and then treated with 8 mM ebselen for 48 h. Each experiment was repeated at least three times ($n = 3$)

TNF and IL-6. As shown in Fig. 2B,C, the expression of IL-6 and TNF-β in the H1N1 group was elevated compared with the control group, indicating that during H1N1 infection, these cytokines showed significant effect as inflammatory mediators. After treatment with ebselen, the expressions of these inflammatory mediators were decreased. In general, these findings demonstrated that ebselen inhibited the inflammatory response caused by H1N1 infection.

Effect of Ebselen in Virus-induced Apoptosis

Annexin-V/PI staining was used to detect the effect of ebselen on virus-mediated apoptosis. As shown in Fig. 3A, compared with the control, the percentages of apoptotic cells at early and late stages in the H1N1 groups were 23.37% and 25.83%, respectively. And the percentage of alive cells declined to only 48.27%. Nevertheless, in the H1N1 + ebselen group, the proportion of early and late apoptotic cells was 7.89% and 12.34%. In contrast, the percentage of alive cells was significantly enhanced (73.29%). As shown in Fig. 3B, the intensities of red fluorescence (propidium iodide positive) and green fluorescence (Annexin-V positive) in the ebselen + H1N1 group decreased, indicating that ebselen inhibited H1N1-induced apoptosis of MDCK cells.

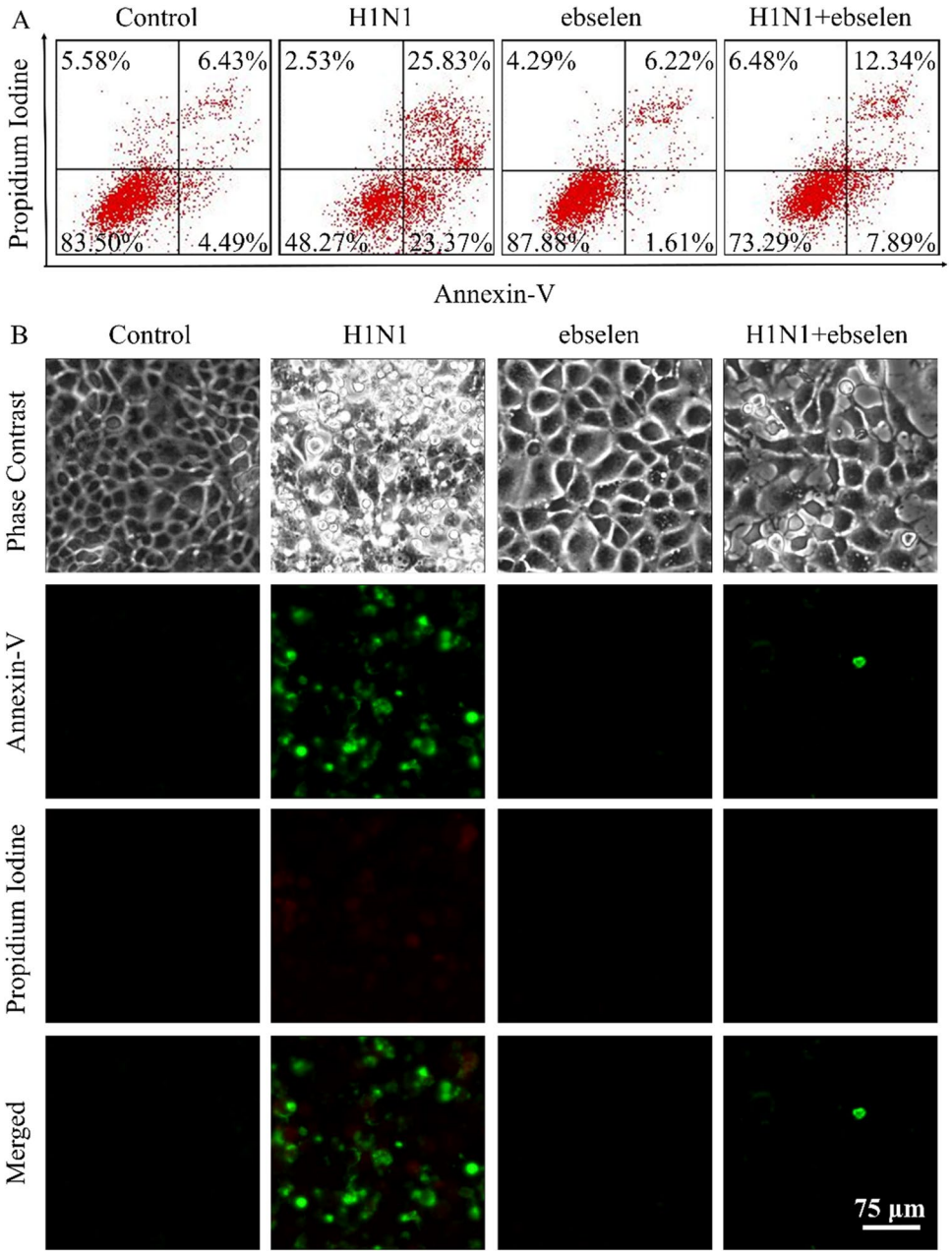

Fig. 3 Ebselen inhibited the apoptosis of MDCK cells induced by H1N1 infection. (**A**) Apoptosis of MDCK cells after different treatments was detected by Annexin-V/PI staining. (**B**) Apoptosis of MDCK cells was detected by Annexin–V/PI staining assay and photographed by fluorescence microscope. The titer of H1N1 was 100 $TCID_{50}$/0.1 mL. MDCK cells were infected with H1N1 for 2 h and then treated with 8 mM ebselen for 48 h. Each experiment was repeated at least three times ($n=3$)

Cell Cycle Changes and DNA Fragmentation Mediated by H1N1 were Inhibited by Ebselen

The cell cycle was measured to assess the impact of ebselen on the cell cycle distribution of virus-infected MDCK cells. As shown in Fig. 4A, the DNA of the control group was mainly distributed in G0/G1 stage. After viral infection, the distribution of sub-G1 peaks in the histogram significantly increased, and the percentage of apoptotic cells was 22.6%. After ebselen treatment, the percentage declined to 8.7%, thus indicating that ebselen inhibited H1N1-induced cell apoptosis. Mitochondrial damage usually leads to the retardation of the intracellular redox reaction process, which causes damage to intracellular macromolecules such as nucleic acids. In addition, early apoptosis is characterized by DNA breakage and nuclear pyknosis, which occur earlier than the change of cell morphology. As shown in Fig. 4B, compared with the control group, DNA fragments increased in the H1N1 infected group, and the nucleus was pyknotic. After treatment with ebselen, the characteristics of apoptosis were significantly reduced. More precisely, nuclear morphologic changes and DNA damage were reduced, suggesting that ebselen inhibited virus-induced DNA damage in MDCK cells.

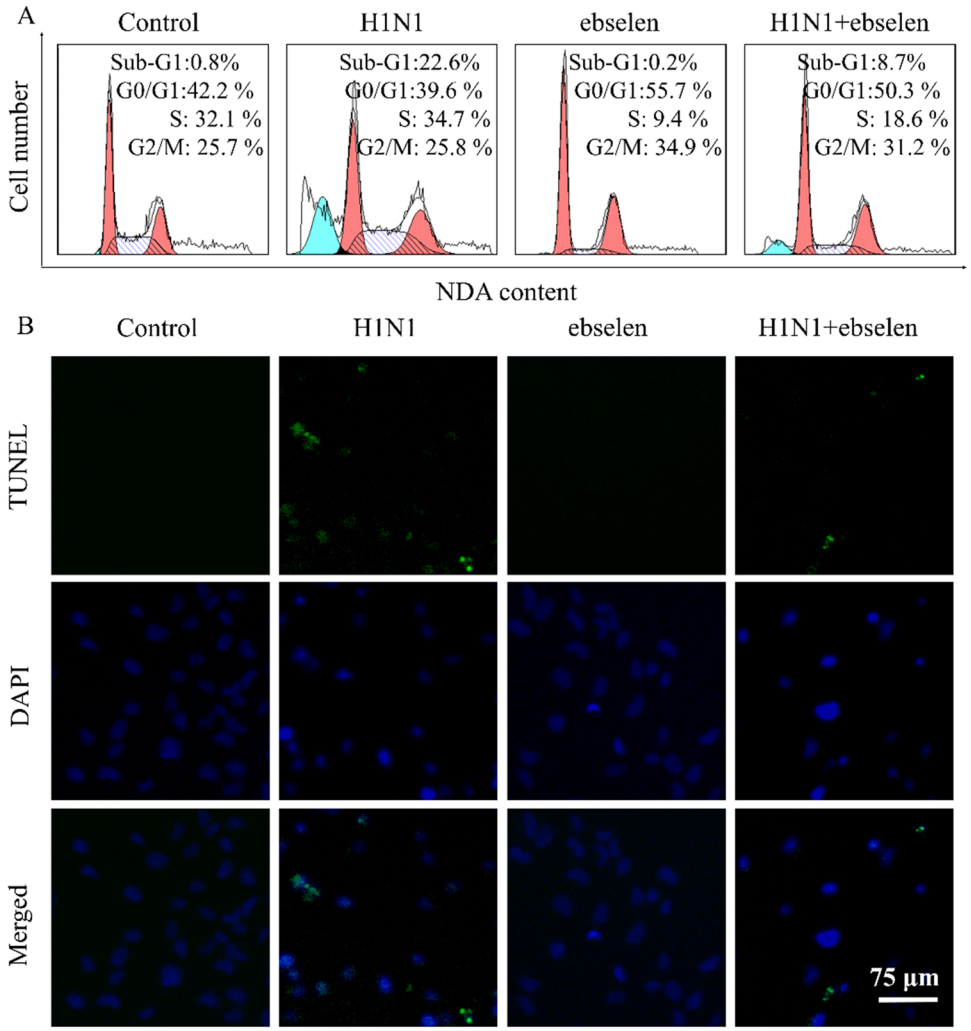

Fig. 4 Ebselen inhibited the cell cycle changes and DNA fragmentation mediated by H1N1. (**A**) The cell cycle of MDCK after different treatments were determined by flow cytometry. (**B**) DNA fragments and nuclear condensation of MDCK cells after different treatments were detected by TUNEL-DAPI staining. The titer of H1N1 was 100 $TCID_{50}$/0.1 mL. MDCK cells were infected with H1N1 for 2 h and then treated with 8 mM ebselen for 48 h. Each experiment was repeated at least three times ($n = 3$)

Changes of Mitochondrial Membrane Potential by Ebselen

One of the initiating mechanisms of apoptosis is the decline of mitochondrial membrane potential (MMP). When the mitochondrial membrane depolarized, JC-1 changed from polymer to monomer. In this study, JC-1 fluorescent probe was used to detect the change of membrane potential of MDCK cells infected with H1N1 after ebselen treatment. As shown in Fig. 5, the number and intensity of JC-1 positive monomer (green fluorescence) in the H1N1 infected group were significantly increased compared with the control group. However, after treatment with ebselen, mitochondrial depolarization was reduced and red fluorescence was enhanced, suggesting that ebselen could inhibit mitochondrial dysfunction induced by H1N1 and prevent cell apoptosis.

Inhibition of ROS Production Mediated by H1N1 by Ebselen

Influenza infection-mediated decline in mitochondrial membrane potential causes the accumulation of ROS, which leads to nucleic acid fragmentation. In order to verify whether mitochondrial ROS production has an impact on nucleic acid fragmentation, ROS kits were used to evaluate the production of ROS in cells after H1N1 infection. As shown in Fig. 6A, ROS levels in the H1N1 group were 275%, significantly higher than in the control group. As exhibited in Fig. 6B, compared with the control group, the green fluorescence of the infected H1N1 group was more obvious. However, the green fluorescence intensity decreased significantly after treatment with ebselen. These results suggested that ebselen inhibited the production of ROS induced by H1N1.

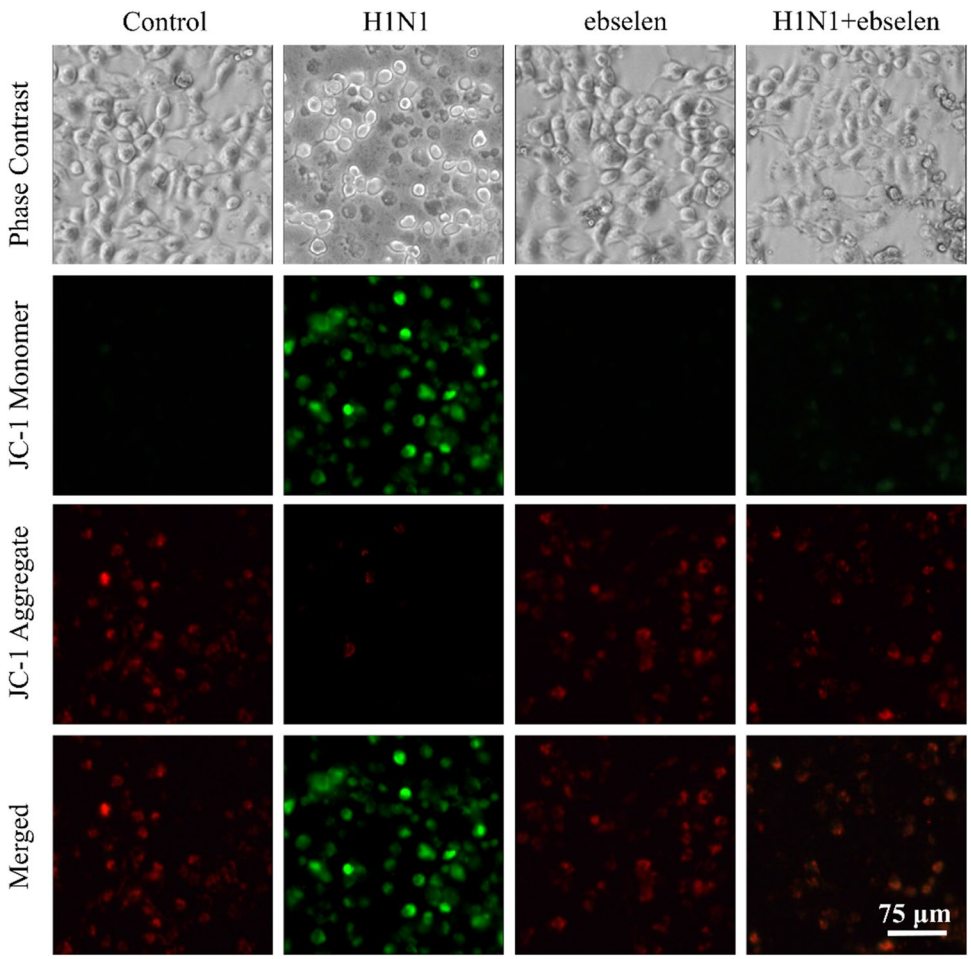

Fig. 5 Changes in mitochondrial membrane potential of MDCK cells after different treatments were detected by the JC-1 kit. The titer of H1N1 was 100 $TCID_{50}$/0.1 mL. MDCK cells were infected with H1N1 for 2 h and then treated with 8 mM ebselen for 48 h. Each experiment was repeated at least three times ($n = 3$)

Ebselen Modulated the ATM/ATR Signal Pathway

The mechanism of viral apoptosis by ebselen was further investigated. As shown in Fig. 7A, H1N1 viral infection induced the increased expression of P-ATM and P-ART and activated the ATM/ATR signal pathway compared with the controls. However, compared with the virus group, the expressions of P-ATM and P-ATR in the H1N1 + ebselen group were reduced, thus indicating that ebselen inhibited H1N1-induced cellular apoptosis by down-regulating ROS-mediated ATM/ATR signal pathway (Fig. 7B). Meanwhile, the expression of Cleave PARP and Cleave Caspase-3 increased in the H1N1 group, but decreased after ebselen treatment (Fig. 7A). It can be speculated that viral infection leads to more PARP cleavage and thus activation of the apoptotic executive protein Caspase-3 (Fig. 7B). β-actin was used as an internal reference for protein expression.

Discussion

Although the anti-influenza effect of ebselen has been confirmed in some studies [21], its antiviral mechanism has not been clearly defined. Ebselen has glutathione peroxidase activity, which can play a certain antioxidant role in cells. In this work, the anti-influenza effect and anti-influenza mechanism of ebselen were studied and verified. Ebselen was identified for the first time as an inhibitor of apoptosis and inflammation associated with influenza-mediated oxidative damage. The anti-influenza mechanism of ebselen was further elaborated.

Ebselen is a small molecule with glutathione-like peroxidase activity, and the antioxidant activity of glutathione peroxidase is closely related to the oxidative damage caused by influenza infection [31–33]. Ebselen has been reported to have a certain anti-influenza effect, but it has not been determined whether its anti-influenza mechanism is related to antioxidant activity. In this work, the anti-influenza effect and inhibition of influenza replication of ebselen were verified by CCK-8, confirming the authenticity of previous reports. Subsequently, ebselen was shown to inhibit influenza virus-mediated apoptosis by cell cycle assay. Annexin-V/PI double staining confirmed that influenza-induced apoptosis and that ebselen inhibited it.

Further exploring how ebselen influenza mediates cell apoptosis, it was found that ebselen could improve the virus-induced decline in mitochondrial membrane potential. In

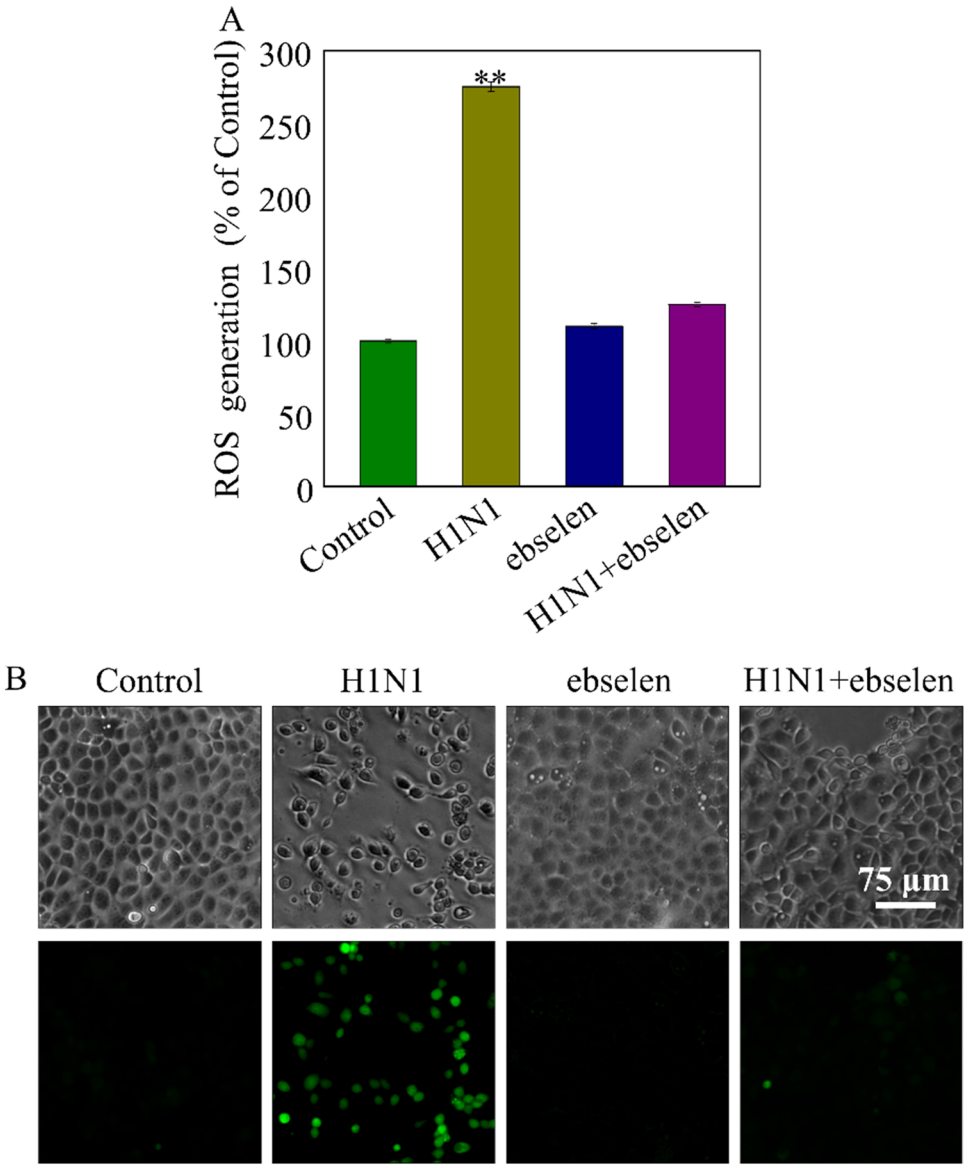

Fig. 6 The inhibition of ROS production induced by ebselen in MDCK cells infected with H1N1. (**A**) The fluorescence intensity of intracellular DCF was measured with a microplate analyzer to reflect the production of ROS. (**B**) ROS levels were captured by a fluorescence microscope. The titer of H1N1 was 100 $TCID_{50}$/0.1 mL. MDCK cells were infected with H1N1 for 2 h and then treated with 8 mM ebselen for 48 h. Each experiment was repeated at least three times ($n=3$)

general, the decrease of mitochondrial membrane potential is closely related to the imbalance of intracellular redox reactions [34, 35]. However, the imbalance of redox is bound to lead to the accumulation of ROS [36], resulting in the damage of intracellular biological macromolecules, such as nucleic acid fragmentation and protein degeneration [37]. Therefore, TUNEL-DAPI staining was used to detect DNA damage in cells after virus infection [38]. Ebselen was found to inhibit DNA damage in virus-infected cells. The reason is that ebselen reduces the accumulation of virus-mediated ROS, thereby preventing ROS damage. In-depth studies of influenza-mediated apoptosis have shown that viral infection leads to the activation of ATM and ATR signaling pathways [39]. In addition, ATM phosphorylation results in the cleavage of downstream PARP and activation of apoptotic executive protein Caspase-3 [40, 41]. Ebselen inhibited p-ATM and P-ATR, thus inhibiting the activation of PARP and Caspase-3 and avoiding apoptosis.

In addition, ebselen also plays a role in the inflammatory response caused by influenza. The viral infection leads to an increase in the release of inflammatory factors such as TNF-β and IL-6 [42–44]. After treatment with ebselen, the release of pro-inflammatory cytokines from influenza-infected cells was reduced. Ebselen reduced virus-mediated inflammation.

Conclusion

It was confirmed that the anti-influenza mechanism of ebselen was realized by inhibiting cell apoptosis mediated by H1N1. By regulating apoptotic proteins, ebselen alleviated

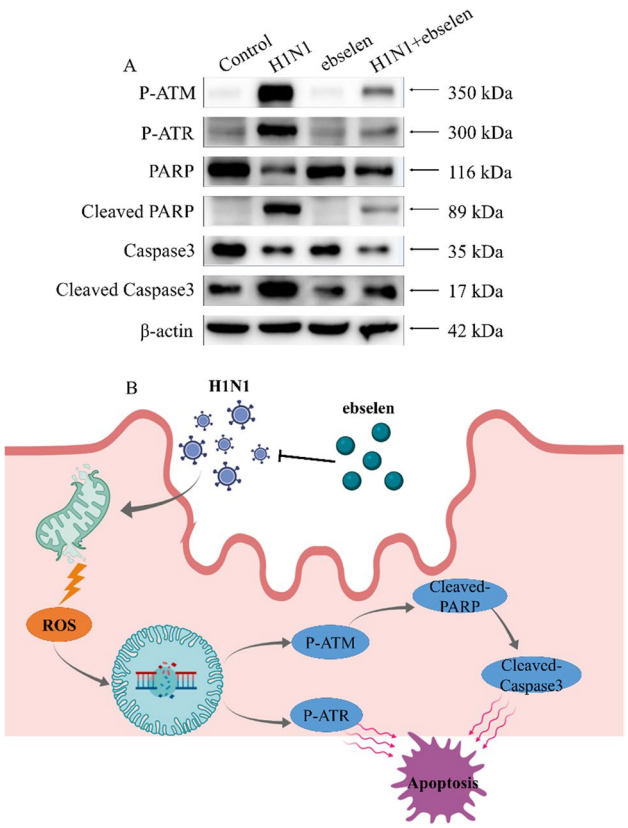

Fig. 7 Signaling pathway participated in the inhibition of H1N1 by ebselen. (**A**) Regulation of apoptotic proteins. (**B**) Scheme of apoptosis signaling pathways. The titer of H1N1 was 100 $TCID_{50}$/0.1 mL. MDCK cells were infected with H1N1 for 2 h and then treated with 8 mM ebselen for 48 h. After that, MDCK cells were lysed with RIPA lysate. Each experiment was repeated at least three times ($n = 3$)

the decline of mitochondrial membrane potential caused by influenza, inhibited the accumulation of ROS caused by mitochondrial damage, and reduced DNA fragmentation of influenza-infected cells, thus inhibiting cell apoptosis. On the other hand, ebselen regulated the release of intracellular pro-inflammatory factors and alleviated the influenza-mediated inflammatory response. However, the anti-influenza mechanism of ebselen needs further study, and the relationship between its antioxidant activity and influenza-mediated oxidative damage needs further elucidation. In conclusion, ebselen is a promising antiviral drug.

Acknowledgements This work was supported by the fund from the Open Project of Guangdong Key Laboratory of Marine Materia (LMM2020-7), the technology planning projects of Guangzhou (202201020655 and 202102010202), the Guangdong Natural Science Foundation (2020A1515110648), the Open Fund of Guangdong Provincial Key Laboratory of Functional Supramolecular Coordination Materials and Applications (2020A03), and the Guangzhou Medical University Students' Science and Technology Innovation Project (2021AEK119, 2021AEK122, 2021AEK125, 2021AEK128 and 02-408-2203-2079).

Author Contribution Danyang Chen, Ruilin Zheng, and Jingyao Su designed the study, analyzed the experimental data, and drafted the manuscript. Jia Lai and Haitian Chen carried out the experiments. Zhihui Ning and Xia Liu analyzed the data. Bing Zhu and Yinghua Li refined the manuscript and coordinated the study. All authors read and approved the final manuscript.

Declarations

Human and Animal Rights This article does not contain any studies with human or animal subjects performed by any of the authors.

Conflict of Interest The authors declare no competing financial interest.

References

1. Javanian M, Barary M, Ghebrehewet S, Koppolu V, Vasigala V, Ebrahimpour S (2021) A brief review of influenza virus infection. J Med Virol 93(8):4638–4646. https://doi.org/10.1002/jmv.26990
2. Bailey ES, Choi JY, Fieldhouse JK, Borkenhagen LK, Zemke J, Zhang D (2018) Gray GC (2018) The continual threat of influenza virus infections at the human-animal interface: what is new from a one health perspective? Evol Med Public Health 1:192–198. https://doi.org/10.1093/emph/eoy013
3. Krammer F, Smith G, Fouchier R, Peiris M, Kedzierska K, Doherty PC, Palese P, Shaw ML, Treanor J, Webster RG, Garcia-Sastre A (2018) Influenza. Nat Rev Dis Primers 4(1):3. https://doi.org/10.1038/s41572-018-0002-y
4. Peteranderl C, Herold S, Schmoldt C (2016) Human influenza virus infections. Semin Respir Crit Care Med 37(4):487–500. https://doi.org/10.1055/s-0036-1584801
5. Nachbagauer R, Palese P (2020) Is a universal influenza virus vaccine possible? Annu Rev Med 71(1):315–327. https://doi.org/10.1146/annurev-med-120617-041310
6. Krammer F (2016) Novel universal influenza virus vaccine approaches. Curr Opin Virol 17:95–103. https://doi.org/10.1016/j.coviro.2016.02.002
7. Ison MG (2017) Antiviral treatments. Clin Chest Med 38(1):139–153. https://doi.org/10.1016/j.ccm.2016.11.008
8. Lampejo T (2020) Influenza and antiviral resistance: an overview. Eur J Clin Microbiol Infect Dis 39(7):1201–1208. https://doi.org/10.1007/s10096-020-03840-9
9. Tilmanis D, Koszalka P, Barr IG, Rossignol JF, Mifsud E, Hurt AC (2020) Host-targeted nitazoxanide has a high barrier to resistance but does not reduce the emergence or proliferation of oseltamivir-resistant influenza viruses in vitro or in vivo when used in combination with oseltamivir. Antiviral Res 180:104851. https://doi.org/10.1016/j.antiviral.2020.104851
10. Yen HL, Mckimm-Breschkin JL, Choy KT, Wong DD, Cheung PP, Zhou J, Ng IH, Zhu H, Webby RJ, Guan Y, Webster RG, Peiris JS (2013) Resistance to neuraminidase inhibitors conferred by an R292K mutation in a human influenza virus H7N9 isolate can be masked by a mixed R/K viral population. Mbio 4(4) https://doi.org/10.1128/mBio.00396-13
11. Tandel K, Sharma S, Dash PK, Parida M (2018) Oseltamivir-resistant influenza A(H1N1)pdm09 virus associated with high case fatality, India 2015. J Med Virol 90(5):836–843. https://doi.org/10.1002/jmv.25013
12. To EE, Erlich JR, Liong F, Luong R, Liong S, Esaq F, Oseghale O, Anthony D, Mcqualter J, Bozinovski S, Vlahos R, O'Leary JJ, Brooks DA, Selemidis S (2020) Mitochondrial reactive oxygen

species contribute to pathological inflammation during influenza A virus infection in mice. Antioxid Redox Signal 32(13):929–942. https://doi.org/10.1089/ars.2019.7727
13. Di Meo S, Reed TT, Venditti P, Victor VM (2016) Role of ROS and RNS sources in physiological and pathological conditions. Oxid Med Cell Longev 2016:1245049. https://doi.org/10.1155/2016/1245049
14. Zorov DB, Juhaszova M, Sollott SJ (2014) Mitochondrial reactive oxygen species (ROS) and ROS-induced ROS release. Physiol Rev 94(3):909–950. https://doi.org/10.1152/physrev.00026.2013
15. Srinivas US, Tan B, Vellayappan BA, Jeyasekharan AD (2019) ROS and the DNA damage response in cancer. Redox Biol 25:101084. https://doi.org/10.1016/j.redox.2018.101084
16. Li Y, Lin Z, Guo M, Zhao M, Xia Y, Wang C, Xu T, Zhu B (2018) Inhibition of H1N1 influenza virus-induced apoptosis by functionalized selenium nanoparticles with amantadine through ROS-mediated AKT signaling pathways. Int J Nanomedicine 13:2005–2016. https://doi.org/10.2147/IJN.S155994
17. Li Y, Lin Z, Guo M, Xia Y, Zhao M, Wang C, Xu T, Chen T, Zhu B (2017) Inhibitory activity of selenium nanoparticles functionalized with oseltamivir on H1N1 influenza virus. Int J Nanomedicine 12:5733–5743. https://doi.org/10.2147/IJN.S140939
18. Guo XJ, Thomas PG (2017) New fronts emerge in the influenza cytokine storm. Semin Immunopathol 39(5):541–550. https://doi.org/10.1007/s00281-017-0636-y
19. Zou L, Lu J, Wang J, Ren X, Zhang L, Gao Y, Rottenberg ME, Holmgren A (2017) Synergistic antibacterial effect of silver and ebselen against multidrug-resistant Gram-negative bacterial infections. Embo Mol Med 9(8):1165–1178. https://doi.org/10.15252/emmm.201707661
20. Simanjuntak Y, Liang JJ, Chen SY, Li JK, Lee YL, Wu HC, Lin YL (2018) Ebselen alleviates testicular pathology in mice with Zika virus infection and prevents its sexual transmission. Plos Pathog 14(2):e1006854. https://doi.org/10.1371/journal.ppat.1006854
21. Oostwoud LC, Gunasinghe P, Seow HJ, Ye JM, Selemidis S, Bozinovski S, Vlahos R (2016) Apocynin and ebselen reduce influenza A virus-induced lung inflammation in cigarette smoke-exposed mice. Sci Rep 6:20983. https://doi.org/10.1038/srep20983
22 Chen YW, Yiu CB, Wong KY (2020) Prediction of the SARS-CoV-2 (2019-nCoV) 3C-like protease (3CL (pro)) structure: virtual screening reveals velpatasvir, ledipasvir, and other drug repurposing candidates. F1000Res 9:129. https://doi.org/10.12688/f1000research.22457.2
23. Lei C, Yang J, Hu J, Sun X (2021) On the calculation of TCID50 for quantitation of virus infectivity. Virol Sin 36(1):141–144. https://doi.org/10.1007/s12250-020-00230-5
24. Najar B, Nardi V, Stincarelli MA, Patrissi S, Pistelli L, Giannecchini S (2021) Screening of the essential oil effects on human H1N1 influenza virus infection: an in vitro study in MDCK cells. Nat Prod Res:1–4. https://doi.org/10.1080/14786419.2021.1944137
25. Wang C, Chen H, Chen D, Zhao M, Lin Z, Guo M, Xu T, Chen Y, Hua L, Lin T, Tang Y, Zhu B, Li Y (2020) The inhibition of H1N1 influenza virus-induced apoptosis by surface decoration of selenium nanoparticles with beta-Thujaplicin through reactive oxygen species-mediated AKT and p53 signaling pathways. ACS Omega 5(47):30633–30642. https://doi.org/10.1021/acsomega.0c04624
26. Chen Z, Chen J, Wei X, Hua H, Hu R, Ding N, Zhang J, Song D, Ye Y, Tang Y, Ding Z, Ke S (2021) Antiviral activities of carbazole derivatives against porcine epidemic diarrhea virus in vitro. Viruses 13(12) https://doi.org/10.3390/v13122527
27. Lin Z, Li Y, Gong G, Xia Y, Wang C, Chen Y, Hua L, Zhong J, Tang Y, Liu X, Zhu B (2018) Restriction of H1N1 influenza virus infection by selenium nanoparticles loaded with ribavirin via resisting caspase-3 apoptotic pathway. Int J Nanomedicine 13:5787–5797. https://doi.org/10.2147/IJN.S177658
28. Li Y, Lin Z, Zhao M, Xu T, Wang C, Hua L, Wang H, Xia H, Zhu B (2016) Silver nanoparticle based codelivery of oseltamivir to inhibit the activity of the H1N1 influenza virus through ROS-mediated signaling pathways. ACS Appl Mater Interfaces 8(37):24385–24393. https://doi.org/10.1021/acsami.6b06613
29. Crowley LC, Marfell BJ, Scott AP, Waterhouse NJ (2016) Quantitation of apoptosis and necrosis by annexin V binding, propidium iodide uptake, and flow cytometry. Cold Spring Harb Protoc 2016(11) https://doi.org/10.1101/pdb.prot087288
30. Park JW, Hong SP, Lee JH, Moon SH, Cho YS, Jung KH, Lee J, Lee KH (2020) 99mTc-MIBI uptake as a marker of mitochondrial membrane potential in cancer cells and effects of MDR1 and verapamil. PLoS One 15(2):e228848. https://doi.org/10.1371/journal.pone.0228848
31. Guillin OM, Vindry C, Ohlmann T, Chavatte L (2019) Selenium, selenoproteins and viral infection. Nutrients 11(9) https://doi.org/10.3390/nu11092101
32. Checconi P, De Angelis M, Marcocci ME, Fraternale A, Magnani M, Palamara AT, Nencioni L (2020) Redox-modulating agents in the treatment of viral infections. Int J Mol Sci 21(11) https://doi.org/10.3390/ijms21114084
33. Yatmaz S, Seow HJ, Gualano RC, Wong ZX, Stambas J, Selemidis S, Crack PJ, Bozinovski S, Anderson GP, Vlahos R (2013) Glutathione peroxidase-1 reduces influenza A virus-induced lung inflammation. Am J Respir Cell Mol Biol 48(1):17–26. https://doi.org/10.1165/rcmb.2011-0345OC
34. Kalpage HA, Bazylianska V, Recanati MA, Fite A, Liu J, Wan J, Mantena N, Malek MH, Podgorski I, Heath EI, Vaishnav A, Edwards BF, Grossman LI, Sanderson TH, Lee I, Huttemann M (2019) Tissue-specific regulation of cytochrome c by post-translational modifications: respiration, the mitochondrial membrane potential, ROS, and apoptosis. Faseb J 33(2):1540–1553. https://doi.org/10.1096/fj.201801417R
35. Suski JM, Lebiedzinska M, Bonora M, Pinton P, Duszynski J, Wieckowski MR (2012) Relation between mitochondrial membrane potential and ROS formation. Methods Mol Biol 810:183–205. https://doi.org/10.1007/978-1-61779-382-0_12
36. Ruankham W, Suwanjang W, Phopin K, Songtawee N, Prachayasittikul V, Prachayasittikul S (2021) Modulatory effects of alpha-mangostin mediated by SIRT1/3-FOXO3a pathway in oxidative stress-induced neuronal cells. Front Nutr 8:714463. https://doi.org/10.3389/fnut.2021.714463
37. Nissanka N, Moraes CT (2018) Mitochondrial DNA damage and reactive oxygen species in neurodegenerative disease. Febs Lett 592(5):728–742. https://doi.org/10.1002/1873-3468.12956
38. Sun W, Li A, Wang Z, Sun X, Dong M, Qi F, Wang L, Zhang Y, Du P (2020) Tetramethylpyrazine alleviates acute kidney injury by inhibiting NLRP3/HIF1alpha and apoptosis. Mol Med Rep 22(4):2655–2664. https://doi.org/10.3892/mmr.2020.11378
39. Jin MH, Oh DY (2019) ATM in DNA repair in cancer. Pharmacol Ther 203:107391. https://doi.org/10.1016/j.pharmthera.2019.07.002
40. Mirza-Aghazadeh-Attari M, Recio MJ, Darband SG, Kaviani M, Safa A, Mihanfar A, Sadighparvar S, Karimian A, Alemi F, Majidinia M, Yousefi B (2021) DNA damage response and breast cancer development: possible therapeutic applications of ATR, ATM, PARP, BRCA1 inhibition. DNA Repair (Amst) 98:103032. https://doi.org/10.1016/j.dnarep.2020.103032

41. Wang XX, Zhang B, Xia R, Jia QY (2020) Inflammation, apoptosis and autophagy as critical players in vascular dementia. Eur Rev Med Pharmacol Sci 24(18):9601–9614. https://doi.org/10.26355/eurrev_202009_23048
42. Racanelli AC, Kikkers SA, Choi A, Cloonan SM (2018) Autophagy and inflammation in chronic respiratory disease. Autophagy 14(2):221–232. https://doi.org/10.1080/15548627.2017.1389823
43. Atri C, Guerfali FZ, Laouini D (2018) Role of human macrophage polarization in inflammation during infectious diseases. Int J Mol Sci 19(6) https://doi.org/10.3390/ijms19061801
44. Hirano T (2021) IL-6 in inflammation, autoimmunity and cancer. Int Immunol 33(3):127–148. https://doi.org/10.1093/intimm/dxaa078